Environ. Sci. Technol. **2006**, *40,* 1231−1236

Diesel Engine Exhaust Emission: Oxidative Behavior and Microstructure of Black Smoke Soot Particulate

J.-O. MÜLLER, D. S. SU,* R. E. JENTOFT, U. WILD, AND R. SCHLÖGL

Department of Inorganic Chemistry (European Laboratory for Catalysis and Surface Science), Fritz-Haber-Institute of the Max-Planck-Society, Faradayweg 4-6, D-14195 Berlin, Germany

Soot particulate collected from a Euro III heavy duty diesel engine run under black smoke conditions was investigated using thermogravimetry, transmission electron microscopy, electron energy loss spectroscopy, and X-ray photoelectron spectroscopy. The characterization results are compared with those of commercial carbon black. The onset temperature toward oxidation of the diesel engine soot in 5% O_2 is 150 °C lower than that for carbon black. The burn out temperature for the diesel engine soot is 60 °C lower than that of the carbon black. The soot primary particles exhibit a core−shell structure. The shell of the soot particles consists of homogeneously stacked basic structure units. The commercial carbon lamp black is more graphitized than the diesel engine soot, whereas the diesel engine soot contains more carbon in aromatic nature than the carbon black and is highly surface-functionalized. Our findings reveal that technical carbon black is not a suitable model for the chemistry of the diesel engine soot.

1 Introduction

Diesel engines have become increasingly used in comparison to spark ignition engines for trucks and passenger cars due to their lower fuel consumption and thus their lower carbon dioxide emissions. The main emission products from diesel engines are carbon dioxide (CO_2), carbon monoxide (CO), hydrocarbons (HC), nitrogen oxides (NO_x), and particulate matter (PM) (*1*). In particular, the high PM content of diesel engine exhaust has been cited as a potential risk to human health (*2*). Epidemiologic and clinical investigations have suggested a strong link between particulate air pollution and, e.g., allergic respiratory disease (*3*).

Many studies indicate that absorbed material in the diesel exhaust PM is responsible for adverse health effects, and smaller particles may have a larger fraction of absorbed material. Furthermore, the composition of diesel exhaust varies with engine loading, and soot from differently loaded engines can have different biological activity (*3*, *4*).

The reactivity of soot particulate with oxygen has been widely investigated to decrease particulate emissions from automobiles, and also from industrial flames. Since the sampling of soot particulate in the amounts required for laboratory scale testing of chemical properties and reactivity is very time-consuming and expensive, commercial carbon black is often used for oxidation or combustion experiments. This substitution is based on the assumption that soot from various sources is structurally similar, and similar to commercial carbon black (*5*−*7*).

In the present work we investigate the oxidation behavior, microstructure, and surface functional groups of the soot particles collected from the raw exhaust of a Euro III stationary heavy duty diesel engine run under black smoke conditions. Such black smoke is emitted when diesel engine fuel combusts under an under-stoichiometric condition (low air/fuel ratio). Thus, the combustion of the diesel engine fuel is not complete resulting in a high concentration of PM in the exhaust. The results of characterization of the diesel engine exhaust soot are compared with those of industrial carbon black. We focus on the structural and chemical differences between the diesel soot and the carbon black and emphasize their microstructure-dependent oxidation behaviors.

2 Experimental Section

The black smoke soot sample (labeled as P1 Soot) originates from the raw exhaust of a Euro III stationary heavy duty Diesel D2876 CR-Engine at 30% load (artificially adjusted for high soot emission by air throttling and reducing rail pressure, blackening number 5). Thus, the combustion of the diesel engine fuel is not complete resulting in a high concentration of PM in the exhaust. The carbon black is a commercially available Lamp Black from Degussa (FR 101 33/D).

The thermogravimetric analysis (TG) was done using a Netzsch-STA 449 instrument with Al_2O_3 crucibles. Because the mass of sample used was very low, and decreases over the experiment until it reaches zero, the reference crucible was left empty. The samples were evacuated and the sample chamber was refilled with 5% O_2 in N_2 which was maintained at a total flow rate of 100 mL/min. The heating rate was 5 K/min. The gas-phase products were transferred through a heated quartz capillary to a Balzers, OmniStar quadrupol mass spectrometer operated in SIM mode. The only products observed were CO_2 (m/e = 44−46) and H_2O (m/e = 17−18). The sample charge used for TG analysis for both samples was about 2 mg. The Lamp Black is denser than the P1 soot; it filled the sample crucible to a lower level.

A Philips CM 200 FEG transmission electron microscope (TEM) equipped with a field emission gun was used to study the morphology and microstructure of the soot. The acceleration voltage was set to 200 kV. EELS spectra were recorded with the Gatan Imaging Filter GIF 100. The energy resolution was 1 eV full width at half-maximum (FWHM) of the zero loss. To avoid any misinterpretation of the image contrast, or the energy loss, all investigations are carried out on soot particles without underlying carbon film.

The X-ray photoelectron spectroscopic (XPS) investigations were carried out in a modified LHS/SPECS EA200 MCD system equipped with facilities for XPS (Mg Kα 1253.6 eV, 168 W power). For the XPS measurements a fixed analyzer pass energy of 48 eV was used resulting in a resolution of 0.9 eV FWHM for the Ag $3d_{5/2}$ peak. The binding energy scale was calibrated using Au $4f_{7/2}$ = 84.0 eV and Cu $2p_{3/2}$ = 932.67 eV. The sample was mounted on a stainless steel sample holder. The base pressure of the UHV analysis chamber was $<1 \times 10^{-10}$ mbar.

3 Results

3.1 Oxidation Experiments. Figure 1 shows TG traces recorded during TPO of the soot samples in 5% O_2 in N_2.

* Corresponding author e-mail: dangsheng@fhi-berlin.mpg.de.

10.1021/es0512069 CCC: $33.50 © 2006 American Chemical Society
Published on Web 01/14/2006

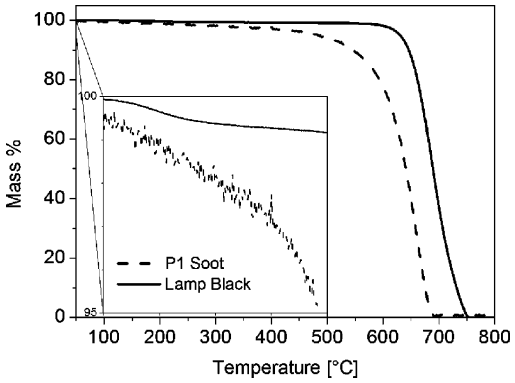

FIGURE 1. TG/TPO experiments on P1 Soot and Lamp Black. The inset shows a magnification of the mass loss over the temperature range from 100 to 500 °C.

The TG signals for both samples remain approximately constant until about 200 °C where the P1 Soot begins to slowly lose mass, losing about 5% by about 450 °C. The rate of mass loss for P1 Soot then increases and reaches a maximum at 660 °C and goes rapidly to zero at about 680 °C. The Lamp Black is more stable than the P1 Soot, losing significant mass beginning only at about 600 °C. The combustion reaches a maximum rate at 700 °C and the Lamp Black is fully consumed by 740 °C. The inset in Figure 1 shows the mass loss at up to 500 °C. The P1 Soot loses 3% of its mass by 450 °C; the Lamp Black loses only 1% of its initial mass by 450 °C.

For both samples, gas analysis shows that the main product is CO_2 with a lesser amount of water. No other gas-phase products are observed. The gas-phase analysis (Figure 2a) shows that the detectable CO_2 evolution for the P1 Soot begins at 400 °C and increases to a maximum at 660 °C. The evolution of water begins at 200 °C and has a local maximum at about 340 °C. This loss of water between 200 and 400 °C is likely from desorption of adsorbed water, dehydroxylation, and decomposition of other functional groups. Above 400 °C the signal for water and the signal for CO_2 increase until they reach a maximum at 660 °C. The ratio of water to CO_2 decreases during this time indicating the oxidation of more highly functionalized species followed by combustion of carbon containing lesser amounts of structural hydrogen. For the Lamp Black, gas-phase products are first detectable at about 550 °C with the appearance of both CO_2 and H_2O. Both gas-phase products show a similar behavior with a maximum concentration at about 700 °C, indicating that the Lamp Black is a more homogeneous material with relatively less functionalization. Integration of the normalized CO_2 signal indicates that there is 10% less carbon per gram of P1 Soot than of the Lamp Black. The respective DSC measurements are displayed in Figure 3. The DSC signals differ in accordance to the different morphologies of the samples. The P1 Soot shows an exothermic DSC signal increasing from the beginning of the experiment which, in part, may represent the heat of combustion of a more highly reactive fraction in the P1 Soot; however, included in this signal is also an artifact caused by the insulating or radiation effect of the black soot on the sample side of the DSC. The DSC signal for P1 Soot ends in a clear exothermic signal with a maximum at 660 °C, corresponding to the maximum rate of mass loss and production of CO_2. The DSC signal returns to zero as the alumina cup is emptied of soot at 680 °C. The DSC signal of the Lamp Black also shows a background signal at low temperature. Since there is no significant mass loss, this signal is completely ascribed to insulating or radiation effects. This background signal is less intense for the denser Lamp Black than for the P1 Soot. Starting at 570 °C there is a broad, nonsymmetric exotherm with a maximum at 700 °C that

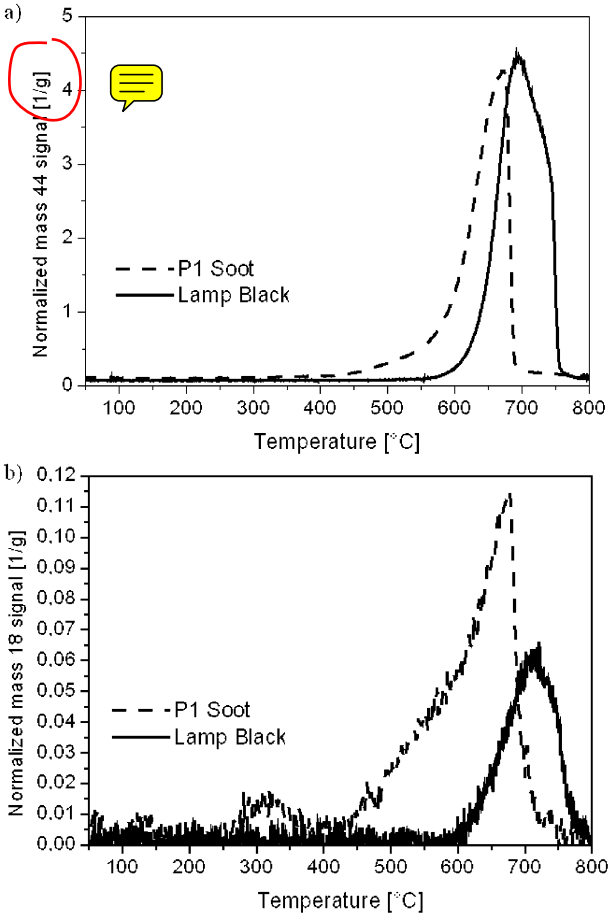

FIGURE 2. Gas evolution from the TPO experiments on P1 Soot and Lamp Black: (a) CO_2 signal, (b) H_2O signal.

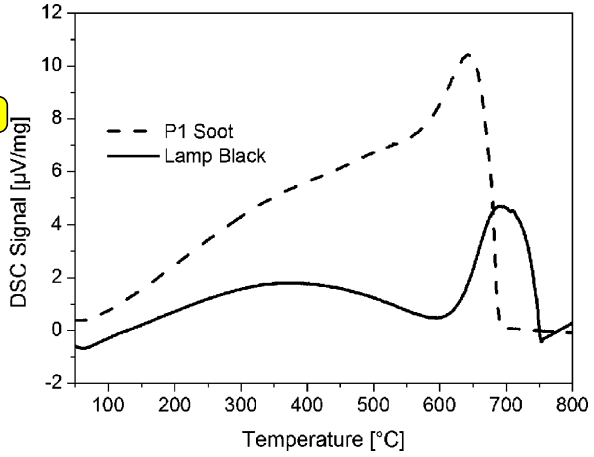

FIGURE 3. DSC measurements on the P1 Soot and the Lamp Black.

correlates to the weight loss and evolution of gas-phase combustion products.

3.2 TEM/HRTEM Measurements. The morphology and microstructure of the P1 Soot and Lamp Black were studied by TEM and HRTEM. The electron micrograph in Figure 4a shows the P1 Soot particulates.The P1 Soot exhibits a secondary structure consisting of a large number of agglomerated spherical particles, a common morphology for soot. The primary particles are homogeneous small particles; the mean size distribution evaluated from TEM is about 25 nm. The agglomerates built up from the spheres have a size from several tens of nanometers to micrometers. The electron micrograph in Figure 4b shows an image of the Lamp Black.

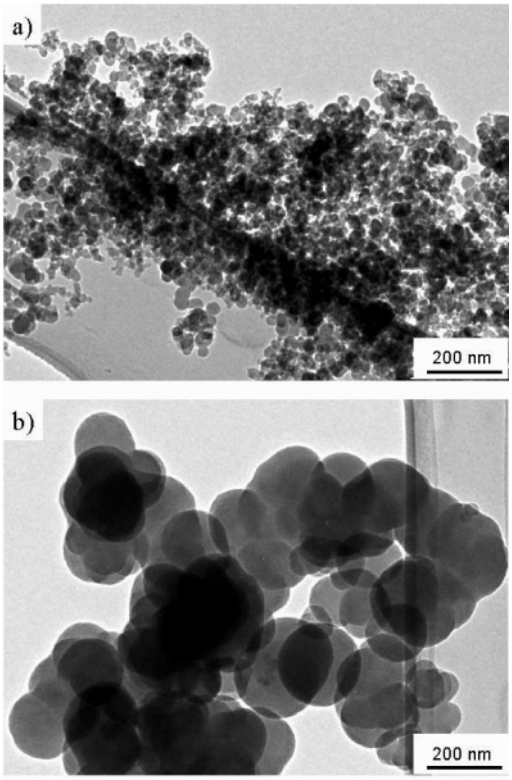

FIGURE 4. TEM micrographs of (a) P1 Soot and (b) Lamp Black.

It consists of primary spherical particles with a broad size distribution having a mean particle size of about 110 nm. In the micrograph large particles with a diameter up to 300 nm are imaged. The Lamp Black primary particles also form agglomerates in a chainlike secondary structure typical for carbon black. The large difference in the size between the primary spherical particles of the soot and of the Lamp Black is mirrored in the differences in surface area. The BET surface area of the P1 Soot (175 m^2/g) is much higher than that of the Lamp Black (11 m^2/g). The microstructure of individual primary particles of the P1 Soot is shown in the high-resolution electron micrograph presented in Figure 5a. The lattice fringe image shows the spherical forms of two primary particles attached to each other. A core−shell structure is visible, which is common for most primary particles. The shell provides a clear lattice fringe contrast from the stacking of the graphene basic structure units (BSU, *8*). The BSUs are of 2−3 nm in size and slightly bent giving the discontinuous fringe contrast in Figure 5a. The BSUs are turbostratically stacked, but inclined in such a way that that the primary particles keep a (nearly) spherical form to minimize surface energy. The core of the P1 Soot does not show any long-range ordered contrast in the high-resolution images. The lack of ordered contrast is consistent with a core composed of disordered, giant polycyclic aromatic hydrocarbons (PAHs) which have been reported to act as nuclei for soot formation (*9*, *10*).

The electron micrograph in Figure 5b reveals the typical microstructure of the outer part of a Lamp Black particle. These particles also consist of homogeneously sized flat BSUs forming large planar graphene layers, some with small curvatures. While P1 Soot particles usually exhibit a shell of less than 10 nm thickness, showing clear fringe contrasts, Lamp Black soot exhibits a fringe contrast region as thick as several tens of nanometers. The Lamp Black soot particles have too large a diameter to allow imaging of clear fringe contrasts from the center of the particles.

3.3 EELS Measurements. EELS spectra were measured to discern the type of carbon to carbon bonding within the

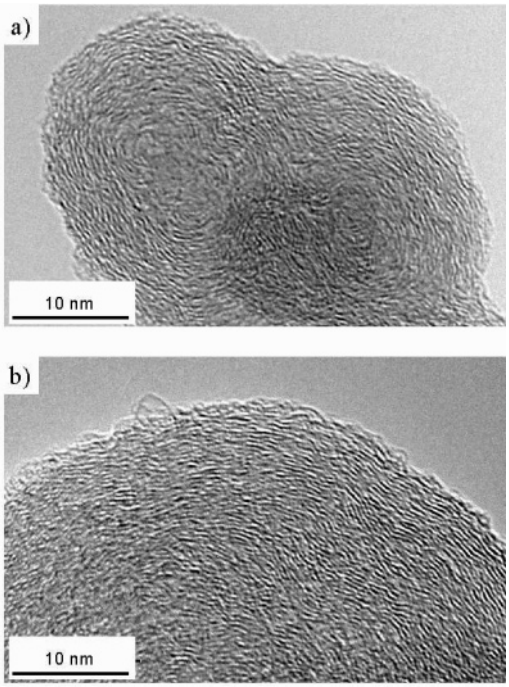

FIGURE 5. HRTEM micrographs of (a) P1 Soot and (b) Lamp Black.

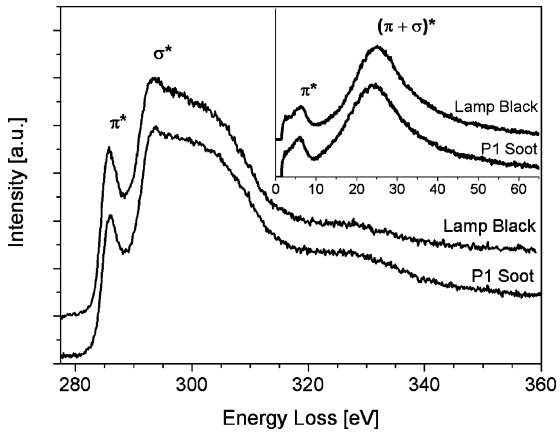

FIGURE 6. Carbon K-ionization edge of P1 Soot and Lamp Black. The inset shows the deconvoluted low-loss spectra.

soot and carbon black samples. The carbon K-ionization edge spectra for the two samples are displayed in Figure 6. The inset in Figure 6 shows the two low-loss spectra acquired from the samples.

The C K-ionization edge shows a distinct maximum at 285 eV which can be attributed to 1s − π^* transitions, and a broad feature from 292 eV to about 313 eV which is attributed to 1s − σ^* transitions. Variation of the intensity at $E = 287 \pm 1$ eV, between these two features, is usually assigned to C−H bond orbitals. The overall lack in fine structure in the σ^*-band (>293 eV) is due to deviation of the structure from perfect graphitic crystals. Nevertheless, the ionization edges reveal differences due to slightly different curvature and predominant bonding. Although the carbon K-ionization edge shows high sp^2 hybridization in both samples, the π^* peak of the P1 Soot has a lower intensity and is broader than that of the Lamp Black. The spectrum of the P1 Soot also has a slightly lower intensity in the first peak at the onset of the σ^* band than does that of the Lamp Black. These differences can be assigned to lower curvature of the graphenes in the Lamp Black, and this is in agreement with our HRTEM observations (Figure 5). It has also been reported that such changes in the C K-ionization edge fine structure are due to

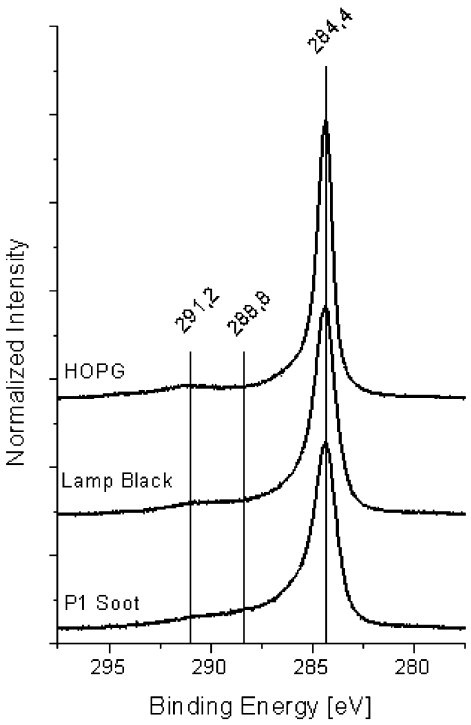

FIGURE 7. XPS measurements: C1s spectra for the P1 Soot and the Lamp Black. The spectra are offset for clarity. For comparison the corresponding spectra of HOPG are included.

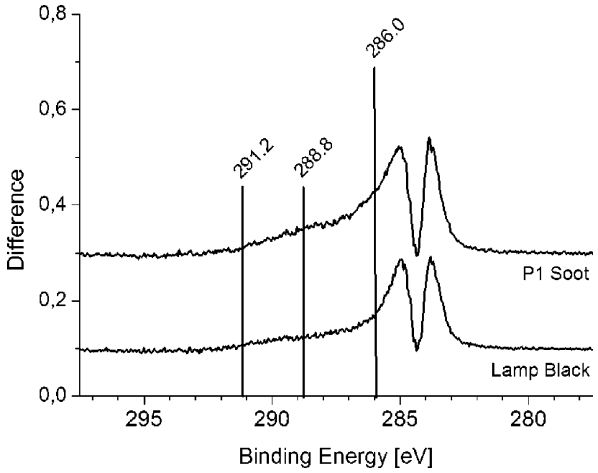

FIGURE 8. Calculated difference spectra for P1 Soot and Lamp Black. The results are offset for clarity.

the presence of carbon-sharing bonds to heteroatoms such as O or H, or from aliphatic chain molecules (*11*).

The inset of Figure 6 shows the low-loss spectra of the investigated materials. The features of the π^* plasmon at 6 eV and the $(\pi + \sigma)^*$ plasmon at 25 eV (P1 Soot) are well developed. The $(\pi+\sigma)^*$ plasmon of the Lamp Black is shifted to a higher energy loss (27 eV). This shift of the $(\pi + \sigma)^*$ plasmon to higher energy loss can be attributed to a difference in the density of valence electrons in the two samples (*12*, *13*), and is indicative of the more complete graphitization of the Lamp Black vs the P1 Soot as seen earlier in the HRTEM images.

3.4 Functional Groups and Surface Composition. Figure 7 and Figure 8 shows C1s and the derived difference spectra for P1 Soot and Lamp Black. Figure 9 shows O1s spectra of P1 Soot and Lamp Black. The spectra of highly ordered pyrolytic graphite (HOPG) are also presented for comparison.

After normalization to the 284.4 eV peak, the spectra of the HOPG was subtracted from the P1 Soot and Lamp Black spectra. The resulting difference spectra are presented in Figure 8. The C1s spectra of both samples (Figure 7) show a maximum in intensity at a binding energy of 284.4 eV. This is an indication for the dominant C−C bonding of the carbon atoms within the particles. This dominant peak is broadened (in comparison to HOPG) due to the defective structure in both samples. It is clear from the intensity at lower energies (E_B < 284.4 eV) in the difference spectra (Figure 8) that the P1 Soot has the broadest fwhm, and this is due to the less developed graphitized structure in comparison to that of the Lamp Black. In both spectra the shake up satellite (291.2 eV) is clearly developed, but less intense than in the spectrum of the HOPG. The lower intensity of the shake up satellite is due to plasmon excitation of the delocalized π electrons in the graphitic structures of the P1 Soot and Lamp Black. Additional intensity at around 286 eV (Figure 8) is attributed to C−H groups present in the samples. The C1s spectrum of the P1 Soot shows an additional shoulder to higher binding energies due to oxygen in surface functional groups. This additional intensity is centered at E_B = 288.8 eV.

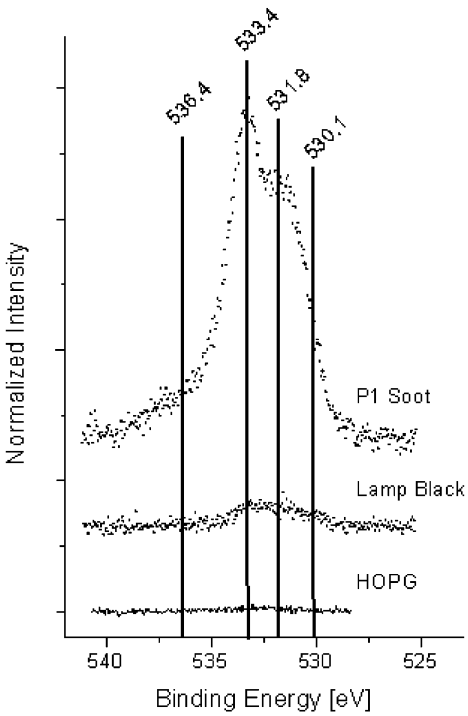

FIGURE 9. XPS measurements: O1s spectra for the P1 Soot and the Lamp Black. The spectra are offset for clarity. For comparison the corresponding spectra of HOPG are included.

The O1s XPS spectra of both samples with the one of HOPG as reference are displayed in Figure 9. While no measurable intensity is recorded on the nonfunctionalized HOPG, the functionalization of the P1 Soot and the Lamp Black is apparent. Both spectra exhibit quite different features and intensities. The O1s spectrum of the P1 Soot has a maximum at 533.4 eV and a plateau centered at 531.8 eV. In addition, there is a small shoulder at about 536.4 eV. Due to the large verity of different oxygen functional groups in these materials (*14*) we did not perform data fitting with Gauss−Lorentz curves. The major components can be assigned as contributions of carbon−oxygen functional groups: C=O at 530.1 eV, C−O−C at 531.8 eV, C−OH at 533.4 eV (*15*−*17*). The shoulder at 536.4 eV is due to differential charging. The O1s spectrum of the P1 Soot shows a tendency to higher binding energies, the weight of the spectrum is at 532.8 eV. The majority of functional groups contain a C−OH group. The broad base indicates a certain amount of differential charging. In the case of the Lamp Black the main contribu-

TABLE 1. Quantification of Surface Oxygen

sample	P1 Soot	lamp black
C	82.6	99.5
O	7.4	0.5

tions arise from C=O and C−O−C configurations, and weight of the spectra is at 531.8 eV. From the areas of the intensities in the C1s and O1s spectra the surface composition of the carbon samples can be calculated and these are presented in Table 1.

4 Discussion

Our relatively simple TG experiments differentiate the P1 Soot (collected from a black smoking Euro III HD diesel engine) from Lamp Black in several ways. First, the P1 Soot is more easily oxidized than the industrial Lamp Black. Second, the extent of the functionalization of the P1 Soot is quantified through integration of the amount of CO_2 evolved. Finally, the desorption of H_2O at about 300 °C indicates the desorption of C−O−H functional groups. The differences in reactivity of the two samples can be explained by their different microstructure and surface functionality. Certainly the small primary particle size (Figure 4) and higher surface area of the P1 Soot may allow higher rates of oxidation of this material than for the Lamp Black. However, the HRTEM micrographs show additional features which will also affect reactivity. The P1 Soot particulate has a core and shell structure. The shell, consisting of stacked, slightly bent graphenes, is much thinner for the P1 Soot than for the Lamp Black. Also, graphenes of the P1 Soot are smaller than those of the Lamp Black and are more strongly bent. The smaller graphenes provide more area for the adsorption of functional groups. The bent graphenes render the structure more prone to the addition of heteroatoms, and thus the reactivity with oxygen is enhanced. This difference in graphitization is also revealed by the EELS measurements. The difference in concentration of heteroatoms correlates well with the results obtained from XPS measurements.

The microstructure and oxidation behavior of soot are determined by the formation processes. Because diesel engines and the composition of diesel fuel are evolving, the relevance of a model soot or model carbon black may be transient. During formation, the spherical P1 Soot particles, with a relatively smooth surface, require a long reaction time to reach this minimum energy situation, or a postsynthetic oxidative episode that burns away surface irregularities. This leaves behind the graphitic layer structure of the outer shell of the primary particles. The graphene layers are short in length, compared with well-crystallized graphite, reflecting the dynamic of soot formation under nonstationary conditions at high pressure and high temperature. Comparing the small spherical particles from the P1 Soot with those from the Lamp Black, apparently, in the generation process of the Lamp Black, the spherical soot particles have a relatively long time to react in order to develop the observed morphology. As seen in the HRTEM micrographs the median size of the Lamp Black particles ranges at ~110 nm, but the particles often exhibit a considerably larger diameter (up to 300 nm). This morphology apparently is the result of a long develop time in a fuel-rich atmosphere. A continuous dehydrogenation of the fuel molecules led to the shell structure consisting of large graphenes with a graphitic structure and a low amount of heteroatoms (hydrogen, oxygen). This is evidenced by the low amount of oxygen as revealed in the XPS measurements.

It is clear that the soot formation conditions control its composition, morphology, and reactivity. We have previously reported that the improved Euro IV diesel engine emits soot containing small fullerenoid particles, a morphology and microstructure due to the technical improvement in engine engineering (*18*). However, the striking results of the present study are the nonnegligible nature of aromatics of the P1 Soot and its high surface functionality. This again makes us aware of the health risks and the environmental threat of black smoke emission in urban traffic. Although the P1 Soot has a higher reactivity toward oxidation compared to the carbon black, its oxidation temperature is still higher than that for the fullerenoid soot of Euro IV diesel engines (*19*, *20*). Additionally, it is clear that while Lamp Black may once have been a suitable model substance for diesel engine soot, this is no longer the case. The developments in diesel engines are changing the soot, and the morphology controlled activity. Certainly the longevity of results from studies will be increased by complete structural characterization and development of structure−reactivity relationships.

In summary the black smoke soot of a test Euro III diesel engine (sample P1 Soot) contains particulate with averaged particle size of 25 nm, agglomerated in a secondary chainlike structure. The primary particles exhibit a core−shell structure and are smaller than those of the commercial Degussa carbon black. The P1 Soot is more aromatic and exhibits higher surface functionality. The oxidation temperature and burning off temperature of the black smoke soot is lower than that of the technical carbon. Our findings reveal that technical carbon black is not a suitable model for the chemistry (and perhaps then the bio-reactivity) of the diesel engine soot. We found a substantial difference between a real soot and particulates that are investigated in great detail.

Acknowledgments

This work is part of the project "Katalytisches System zur filterlosen kontinuierlichen Russpartikelverminderung für Fahrzeugdieselmotoren" supported by the Bayerische Forschungsstiftung and performed in the framework of ELCASS. The authors thank A. Messerer, U. Poschl, and R. Niessner from the TU Munich and D. Rothe and E. Jacob from the MAN Group for instructive discussions and for providing soot samples.

Literature Cited

(1) http://www.dieselnet.com.

(2) USEPA. *2002 Health assessment document for diesel engine exhaust*; Prepared by the National Center for Environmental Assessment, Washington, DC, for the Office of Transportation and Air Quality; EPA/600/8-90/057F; National Technical Information Service: Springfield, VA; PB2002-107661. http://www.epa.gov/ncea.

(3) Riedl, M.; Diaz-Sanchez, D. Biology of diesel exhaust effects on respiratory function. *J. Allergy Clin. Immunol.* **2005**, *115*, 221.

(4) Li, N.; Siutas, C.; Cho, A.; Schmitz, D.; Misra, C.; Sempf, J.; Wang, M.; Oberley, T.; Froines, J.; Nel, A. Ultrafine particulate pollutants induce oxidative stress and mitochondrial damage. *Environ. Health Perspect.* **2003**, *111*, 455.

(5) Jacquot, F.; Logie, V.; Brilhac, J.; Gilot, P. Kinetics of the oxidation of carbon black by NO_2; Influence of the presence of water and oxygen. *Carbon* **2002**, *40*, 335.

(6) Weisweiler, W.; Hizbullah, K.; Kureti, S. Simultaneous Catalytic Conversion of NO_x and Soot from Diesel Engines Exhaust into Nitrogen and Carbon Dioxide. *Chem. Eng. Technol.* **2002**, *25*, 2.

(7) Kureti, S.; Weisweiler, W.; Hizbullah, K. Simultaneous conversion of nitrogen oxides and soot into nitrogen and carbon dioxide over iron containing oxide catalysts in diesel exhaust gas. *Appl. Catal. B* **2003**, *43*, 281.

(8) Oberlin, A. High-Resolution TEM Studies of Carbonization and Graphitization; In *Chemistry and Physics of Carbon 22*; Thrower, P., Ed.; Dekker: New York, 1989.

(9) Ishiguro, T.; Takatori, Y.; Akihama, K. Microstructure of Diesel Soot Particles Probed by Electron Microscopy: First Observation of Inner Core and Outer Shell. *Comb. Flame* **1997**, *108*, 231.

(10) Homann, K.-H. Fullerenes and Soot Formation − New Pathways to Large Particles in Flames. *Angew. Chem., Int. Ed.* **1998**, *37*, 2434.
(11) Braun, A.; Huggins, F. E.; Shah, N.; Chen, Y.; Wirick, S.; Mun, S. B.; Jacobsen, C.; Huffmann, G. P. Advantages of soft X-ray absorption over TEM-EELS for solid carbon studies − a comparative study on diesel soot with EELS and NEXAFS. *Carbon* **2005**, *43*, 117.
(12) Kulik, J.; Lifshitz, Y.; Lempert, G. D.; Rabalais, J. W.; Marton, D. Electron-energy-loss spectroscopy of mass-selected ion-beam-deposited diamondlike carbon. *J. Appl. Phys.* **1994**, *76*, 5063.
(13) Ferrari, A. C.; Libassi, A.; Tanner, B. K.; Stolojan, V.; Yuan, J.; Brown, L. M.; Rodil, S. E.; Kleinsorge, B.; Robertson, J. Density, sp^3 Fraction and Cross-Sectional Structure of Amorphous Carbon Films Determined by X-ray Reflectivity and Electron Energy-Loss Spectroscopy. *Phys. Rev.* **2000**, *B62*, 11089.
(14) Müller, J.-O.; Su, D. S.; Jentoft, R. E.; Kröhnert, J.; Jentoft, F. C.; Schlögl, R. Morphology Controlled Reactivity of Carbonaceous Materials Towards Oxidation. *Catal. Today* **2005**, *102−103*, 259.
(15) Biniak, S.; Szymański, G.; Siedlwski, J.; Światkowski, A. The characterization of activated carbons with oxygen and nitrogen surface groups. *Carbon* **1997**, *35*, 1799.
(16) Boehm, H. P. Surface Oxides on carbon and their analysis: a critical assessment. *Carbon* **2002**, *40*, 145.
(17) Figueiredo, J. L.; Pereira, M. F. R.; Freitas, M. M. A.; Orfao, J. J. M. Modification of the surface chemistry of activated carbons. *Carbon* **1999**, *37*, 1379.
(18) Su, D. S.; Müller, J.-O.; Jentoft, R. E.; Rothe, D.; Jacob, E.; Schlögl, R. Fullerene-like soot from EuroIV diesel engine: consequences for catalytic automotive pollution control. *Topics Catal.* **2004**, *30/31*, 241.
(19) Jacob, E.; Rothe, D.; Schlögl, R.; Su, D. S.; Müller, J.-O.; Niessner, R.; Adelhelm, C.; Messerer, A.; Pöschl, U.; Müllen, K.; Simpson, C.; Tomović, Ž. Dieselruss: Mikrostruktur und Oxidationskinetik. In *24th Internationales Wiener Motorensymposium, 15−16 Mai 2003*; *Band 2: Fortschritt-Berichte VDI Reihe 12 Nr. 539*; Lenz, H. P., Hrsg.; VDI-Verlag: Düsseldorf, 2003; pp 19−45.
(20) Su, D. S.; Jentoft, R. E.; Müller, J.-O.; Rothe, D.; Jacob, E.; Simpson, C. D.; Tomović, Ž.; Müllen, K.; Messerer, A.; Pöschl, U.; Niessner, R.; Schlögl, R. Microstructure and oxidation behavior of Euro IV diesel engine soot: a comparative study with synthetic model soot substances. *Catal. Today* **2004**, *90*, 127.

Received for review June 24, 2005. Revised manuscript received October 20, 2005. Accepted December 5, 2005.

ES0512069